Transaction A: Civil Engineering
Vol. 16, No. 2, pp. 173–187

SCIENTIA IRANICA

Graph Theoretical Topology Control in Structural Optimization of Frames with Bracing Systems

A. Kaveh[1,*] **and M. Shahrouzi**[2]

Abstract. *Many topological objectives and constraints can not easily be assessed by analytical formulations. This paper introduces a number of graph theoretical operators, as suitable combinatorial tools, for discrete topology assessment. Using such an approach, the load paths from their exertion points to the support joints can be guided topologically during the optimization process. Eleven variants of the proposed method are developed for the inclusion of various constraints and/or objectives. The presented algorithms are then applied to the optimal bracing layout of multi-story frames under lateral loadings for minimal weight or static compliance. Benchmark examples from literature are treated to validate the efficiency and to compare the capability of the proposed algorithms. The bracing patterns obtained from optimization are graph theoretically categorized.*

Keywords: *Optimization; Topological assessment; Load path; Graph theory; Super bracing; Frame.*

INTRODUCTION

In order to complete the mathematical design model of a structure under a specified loading state and boundary conditions, the following data packets are required:

1. Structural topology: Connectivity relationship between structural components/members;
2. Structural geometry: The nodal coordinates;
3. Components' shape and sizing: Assignment of structural sections to the members;
4. Material properties: Strength and stiffness characteristics of the utilized material.

The configuration of a structure is defined by its topology, determining the connectivity between structural components. Therefore, it is the most affecting part in the distribution of stiffness/strength and consequent response of the entire structure. The other data, such as section shape and size or the nodal coordinates, are confined to the pre-determined topology as the most important part of the design. On the other hand, such topological information is of a combinatorial nature. The matter is considered as an important reason for the complexity of the structural layout optimization for designers.

The optimal structural design of medium/high rise buildings under seismic or wind loading usually requires employing bracing diagonals in order to keep the inter-story drift values within their desired performance limits. As the topology of a non-braced frame is fixed, the problem will be selection of the best bracing layout in the frame plane among several possible options [1].

Many attempts have already been reported for the topology optimization of trusses [2-5] and the sizing of skeletal frameworks [6-12]. However, for the case of optimal bracing patterns in frames, a few approaches are available [13-15]. Mijar et al. utilized a Voigt-Reuss material mixing rule formulation with a fixed volume fraction constraint [13], while Liang et al. developed a performance-based optimization in an unconstrained form [14,16]. The resulted conceptual designs, as pattern guidelines for an optimal bracing layout, require further interpretation to practical discrete skeletal members and even distributed changes in the original frame design [17]. Each continuum method uses its own way to achieve its final conceptual pattern, which is still an estimate of the discrete optimal topology. However, for a practical design, further considerations should also be considered, such as the buckling-reduced strength of linear members

1. *Department of Civil Engineering, Iran University of Science and Technology, Tehran, P.O. Box 16846-13114, Iran.*
2. *Department of Structural Engineering, Building and Housing Research Center, Tehran, P.O. Box 13145-1696, Iran.*
*. *Corresponding author. E-mail: alikaveh@iust.ac.ir*

Received 1 September 2007; received in revised form 4 December 2007; accepted 17 December 2007

and the desired contribution ratio of certain member types in undergoing lateral loads. This emphasizes the application of a discrete approach in order to achieve the true/practical optimum.

Some topological requirements may not be explicitly formulated by analytical methods. In the case of seismic/wind retrofit, the contribution of existing frame members in the lateral load-resisting system is desired to be minimized [15,18]. This highlights the need to guide the lateral-load paths through bracing members rather than beams and/or columns.

The present work incorporates the graph theory as a powerful tool to handle topological transformations within a deterministic discrete optimization procedure. Special graph theoretical definitions are presented and adopted for an optimal bracing layout. Some final smoothing modifications are then introduced as a partial geometry modifier. Examples of steel multi-story frames are treated from the literature and compared.

AN OVERVIEW OF GRAPH THEORY DEFINITIONS AND OPERATORS

Many graph theoretical concepts applied to structural mechanics can be found in the work of Kaveh [19,20]. Here, only the necessary terms for the present work are introduced and employed in subsequent sections:

1. Graph S consists of a non-empty set $N(S)$ of elements called nodes and a set, $M(S)$, of elements called members, together with a relation of incidence, which associates with each member a pair of nodes called its ends.
2. Two ends of a member are called adjacent to one other and incident to that member. Every two members with a common end are incident members. The degree of a node is the number of members incident to that node.
3. Subgraph S_i of graph S consists of a subset of $N(S_i) \subseteq N(S)$ and a subset of $M(S_i) \subseteq M(S)$, with the members having the same ends as in S.
4. Complete Graph K_n is a graph with n nodes, in which each node is adjacent to all the other $n-1$ nodes.
5. A sequence of alternately non-repeated nodes and members of a graph is called a path. The number of members of a path is defined as the distance between its beginning and end nodes. The graph theoretical length of a member is taken as unity.
6. A graph is called connected, if there is at least one path between every two nodes of the graph.
7. Every maximally connected subgraph of a graph is called its component. A connected graph has only one component.
8. A "Cycle" is a path on which the two end nodes coincide.
9. A "Tree" is a connected graph with no cycle. A tree which contains all the nodes of the graph is called a spanning tree.
10. Considering a specific node in a graph as the root node, a "Shortest Route Tree (SRT)" is defined as a spanning tree in such a parent graph, in which the distance between every node and the root node is minimal. For the formation of a SRT, the root node is labeled the first contour; its adjacent nodes form the second contour and the process is repeated considering the unused adjacent nodes at each step. This procedure is continued until all the nodes are spanned and the SRT is constructed.
11. Multiple Shortest Route Tree (MSRT) is a SRT grown from multiple root nodes.
12. Priority-grown Multiple Shortest Route Tree (PM-SRT) is a subgraph, constructed using the following algorithm:

    Algorithm 1:

    a. Assign the root nodes to the first contour and initialize the SRT node vectors;
    b. Increase the Contour Number (CN) by unity for the new contour;
    c. Enter nodes to the new contour as follows:
        i. Select every node in the previous contour and call it a current parent node.
        ii. Look for any of its adjacent nodes.
        iii. If it is not still labeled and its Priority Number (PN) is greater than the PN of the parent node, label the contour of this node as the new CN. The stem node of this node is the parent node and it is the bud node of that parent.
        iv. Repeat Steps i, ii, iii, until no new adjacent node remains unchecked for labeling in this contour.
    d. Repeat Steps b and c, until there is no other node unchecked for labeling Elements of the vectors; ContourOfNode, StemOf and BudOf should be initiated with a 0-value at the beginning of Step a.

    For the case in which the priority numbers are the same for all the members, the recent algorithm results in a MSRT and if the number of roots is also one, it will represent a SRT.
13. 'Graph Parts (GPs)" are the subsets of graph nodes such that within each subset no node is allowed to be incident to the others.

14. "Adjacent parts" are every two parts of a graph, which consists of at least one node incident to a node in the other part.
15. "Multipartite graph" is a graph which consists of at least two distinct parts.
16. "Frame (associate) graph" is a graph whose members and nodes are in a one-to-one correspondence with the members and the connections of a structural frame, respectively.
17. "Bracing (associate) graph" is a graph whose members and nodes are in a one-to-one correspondence to bracing members and their connections in the structural frame.
18. "Contraction" is replacing a 3-node path with a member connecting the two end nodes of that path.

A typical approach for representing a graph is to denote any kth member by its end nodes (n_i, n_j) and to list all the graph members in a sequence. As an example, the graph of Figure 1a can be represented as: $S = [(n_1, n_2);\ (n_1, n_5);\ (n_1, n_5);\ (n_2, n_3);\ (n_2, n_4);\ (n_2, n_6);\ (n_2, n_7);\ (n_2, n_8);\ (n_3, n_5);\ (n_3, n_7);\ (n_3, n_8);\ (n_4, n_5);\ (n_4, n_7);\ (n_5, n_6);\ (n_5, n_7);\ (n_5, n_8);\ (n_6, n_7);\ (n_6, n_8)]$.

The graph of Figure 1b represents a subgraph of graph S as a path between the following set of nodes: $\{n_4, n_5, n_7, n_3\}$.

The path graph itself is then denoted by: $S_1 = [(n_4, n_5); (n_5, n_7); (n_7, n_3)]$. Its contraction will result in linking (n_4, n_3) as a single member (see Figure 1c).

The 2nd cycle graph in Figure 1d has a node sequence of $\{n_2, n_7, n_5, n_6, n_8, n_3, n_2\}$, in which the first and the last node, n_2, are identical.

Figure 1e shows a tree, which can be a subgraph of S, as its nodes have the same relation of incidence: $S_2 = [(n_1, n_2);\ (n_1, n_5);\ (n_2, n_3);\ (n_2, n_6);\ (n_3, n_8);\ (n_5, n_8)]$.

Two components of graph S_3 in Figure 1f, are represented as S_4 and S_5, where $S_3 = [(n_1, n_5);\ (n_5, n_8);\ (n_2, n_4);\ (n_2, n_6);\ (n_3, n_7);\ (n_4, n_7);\ (n_6, n_7);\ (n_7, n_8)]$, and $S_4 = [(n_1, n_5);\ (n_5, n_8)]$ and $S_5 = [(n_2, n_4);\ (n_2, n_6);\ (n_3, n_7);\ (n_4, n_7);\ (n_6, n_7);\ (n_7, n_8)]$.

A multipartite graph can be considered as the following parts: $\{n_1, n_4\}$, $\{n_2, n_7, n_5\}$ and $\{n_3, n_8, n_6\}$. In which, the following SRT is grown from n_4 as the

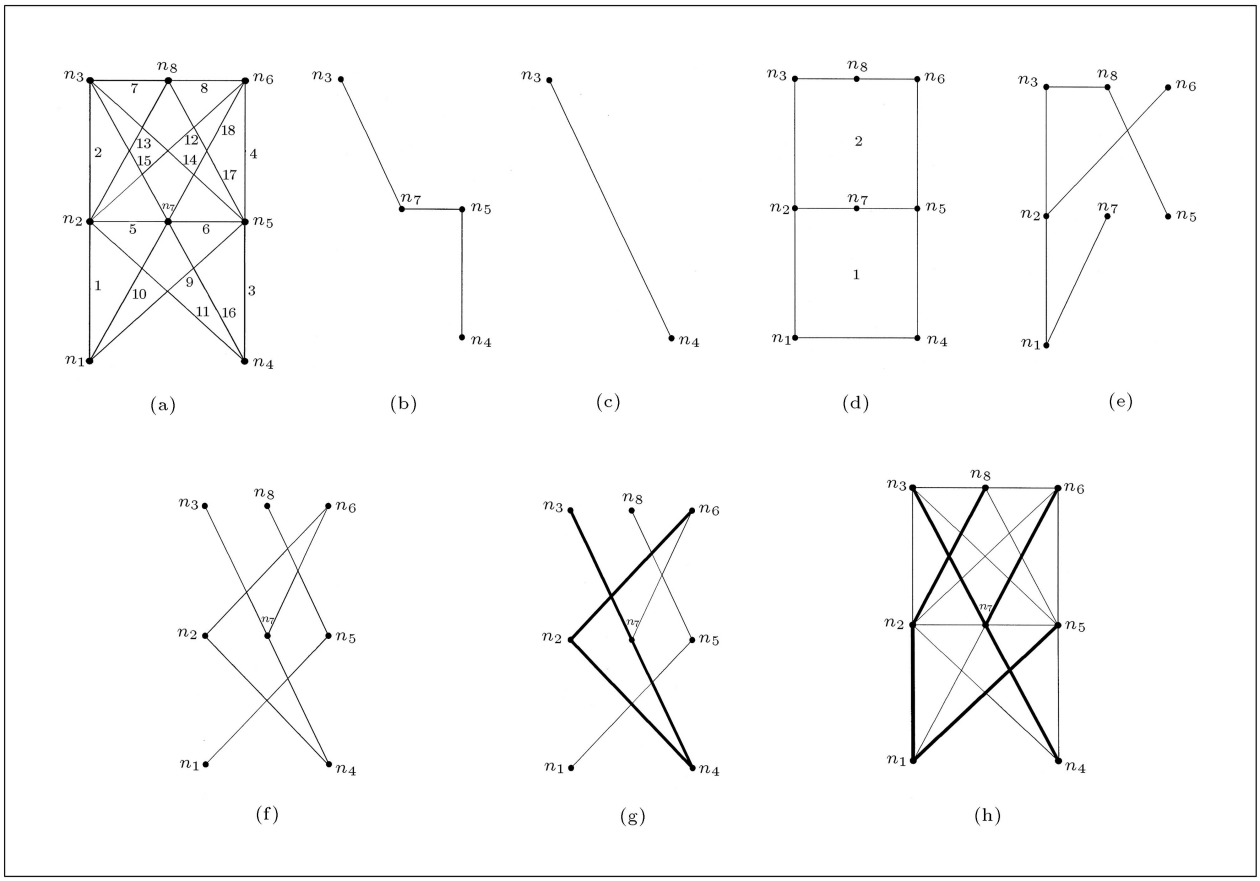

Figure 1. (a) A graph with 8 nodes and 18 members; (b) A path between n_3 and n_4; (c) The contracted form of the path; (d) 2 nested cycle graphs; (e) A typical tree; (f) A multi-partite graph; (g) A SRT rooted from n_4 depicted in bold lines; (h) A MSRT grown from n_1 and n_4 shown in bold lines.

root node in Figure 1g:

$$S_6 = [(n_4, n_2);\ (n_4, n_7);\ (n_2, n_6); (n_7, n_3)].$$

The node set in each contour of such a SRT is determined as:

Contour number 1: $\{n_4\}$;

Contour number 2: $\{n_2, n_7\}$;

Contour number 3: $\{n_3, n_6\}$.

As can be seen, this SRT has covered only one component of S_3, namely S_5.

Figure 1h shows a multiple SRT as a subgraph of S with 2 components; each component is rooted from a distinct node. Thus, there is more than one root node in this MSRT indicated as $\{n_1, n_4\}$, forming the 1st contour of the MSRT. It should be noted that if graph S is associated to a frame with the same topology, the nodes in each identified contour of such MSRT correspond to the nodes at one distinct level of that frame.

GENERATION OF THE PROPER PROTOMORPH

In the topology optimization of skeletal structures, a highly connected initial topology is first generated and the optimal layout is searched via the iterative elimination of less desired members. When such an initial layout is fully connected (similar to a complete graph), it is called the ground structure. From a practical point of view, the ground structure constructed on a frame includes many undesired members, which may arise in the final design. For example, extra generated columns ended between joints of non-neighbor stories. Besides, some diagonal members may interconnect the columns at their mid-height, even if they are forbidden by design codes [21]. A promising technique to prevent such undesired members is to define the search space by a less connected pattern, called protomorph [22], which does not include such undesired members.

Consider a two-bay and six-story building frame, as shown in Figure 2, which has already been treated by a number of investigators [13,14]. Suppose the problem is to find the best bracing layout in such a frame, whereas only concentric V-type bracings are acceptable in the final design and no bracing member is allowed to interconnect a column except at its end joints. For this case, the proper protomorph can be constructed by:

1. Generating the desired number of auxiliary nodes within the length of the beam; e.g. 2 nodes at 1/3 and 2/3 of the length in the example of Figure 2a.
2. Connecting every such node to the neighboring main nodes, i.e. the beam-column joints on the nearest columns and at the lower and higher stories of that bay.

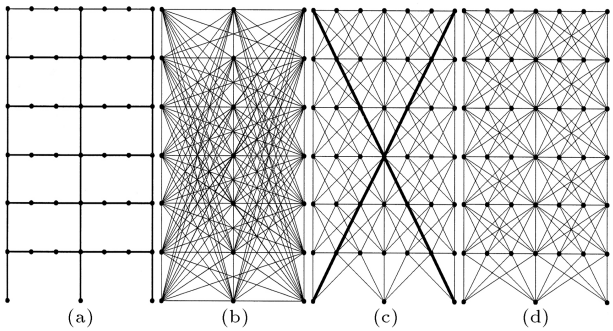

Figure 2. (a) A frame associate graph with 2 auxiliary nodes in each beam; (b) A complete graph associated to the ground structure for a X-braced frame; (c) A protomorph associated to the frame of part (a) and one of its possible super bracing layouts in bold lines; (d) Another protomorph with the additional possibility of every frame opening to be X-braced.

In order to allow the selection of traditional X-bracings, the column ends should also be connected by diagonals. In cases where X-braced spanning of all the 6 stories is an acceptable design alternative, the selected protomorph should include at least two auxiliary intermediate nodes in every beam, as a graph part in the corresponding bracing graph.

Detection of Irregular Topologies During Generation of the Protomorph

In practical design, occasionally, some frame openings forbid the running through of bracings, due to architectural or performance considerations. If effect. In addition to this, the corresponding optimization algorithms may not converge as tested and reported by Mijar et al. [13]. One way to avoid this problem is to detect and prevent the possibility of such topological irregularities by their removal from the protomorph structure, using the following graph theoretical subroutine:

Algorithm 2:

1. Generate all the members of the desired protomorph, except those diagonals such a case leads to a disconnected bracing graph, it may cause a soft-story falling in the forbidden/non-designable openings;
2. Select the support nodes as the set of graph root nodes;
3. Generate a MSRT on the bracing graph, starting from these root nodes;
4. If any diagonal (bracing) member falls outside of the generated MSRT, omit the corresponding member from the protomorph.

Applying the latter algorithm is analogous to omitting any component of the initial bracing graph,

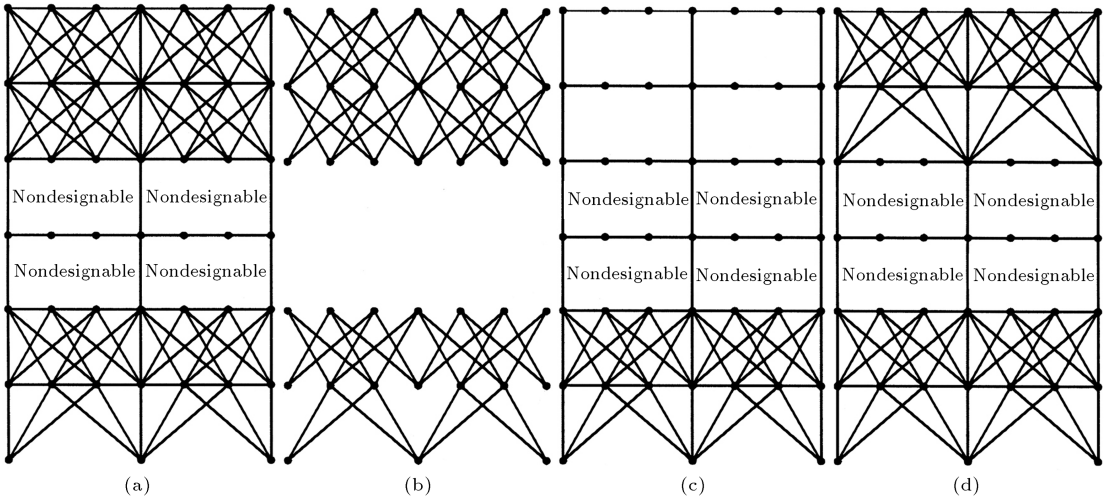

Figure 3. (a) The 3rd and 4th stories as non-designable domains for the bracing layout; (b) Corresponding bracing associate graph and its 2 distinct components; (c) A modified protomorph to avoid the soft story effect; (d) A modified protomorph extracted by removal of members in the upper components, which are incident to auxiliary beam nodes adjacent to the non-designable domain.

except the one including support nodes (Figure 3c). Another modification (Figure 3d) limits the transmission of lateral forces to the upper bracing graph component through columns of non-designable domains.

PROBLEM FORMULATION AND MAIN OPTIMIZATION PROCEDURE

In the present work, the problem of frame bracing layout optimization against static loading $\mathbf{P}$ is formulated as:

$$\text{Minimize } W_b = \rho\ \mathbf{l_b^T}\ \mathbf{A_b}. \tag{1}$$

Subject to:

$$C \leq C_a,$$

with the equality equilibrium constraint:

$$\mathbf{Ku} = \mathbf{P},$$

where:

$\mathbf{A_b} = \{A_1, A_2, 5 \cdots, A_m\}$:	Vector of member cross-sectional areas for bracings;
$\mathbf{l_b} = \{l_1, l_2, \cdots, l_m\}$:	Vector of member lengths for bracings;
$\mathbf{K} = \mathbf{K_f} + \mathbf{K_b}(\mathbf{A_b})$:	Stiffness matrix of the frame and bracing system;
$\mathbf{u}$:	Nodal displacements response;
ρ:	Material density;
$C = \frac{1}{2}\sum_j P_j d_j$:	Mean static compliance along all stories at level number j.

In addition to the main optimization module, a linear elastic structural analysis routine with pre/postprocessor and its required subroutines is programmed to compute the nodal displacement and beam/column/axial-member stress response under equivalent static load cases. In the diaphragm model of floors at a planar frame, the lateral degrees of freedom in nodes at every story level are constrained to each other, so that the corresponding displacement response at the direction of lateral load P_j is calculated as d_j (the jth roof lateral displacement with respect to the basement). When the constant vector of static lateral loads is accepted for being applied as a common practice in designs, due to code-based wind or equivalent seismic loading, the constraint on d vector corresponds to a constraint on mean compliance C. In other words, the equilibrium constraint is implicitly satisfied to compute structural responses.

As mentioned before, deterministic methods of optimization are usually based on the gradual elimination of less efficient members from the initial ground structure or protomorph. Therefore, an element removal criteria measure, η^e, should be first determined. Liang et al. [14] used the element strain energy density, γ^e, for such a measure, based on the sensitivity analysis of the static equilibrium constraint. In this paper, the following Performance Index, PI, is also derived as a modified unconstrained objective function to be maximized:

$$PI^{(i)} = \frac{C^{(0)}.W_b^{(0)}}{C^{(i)}.W_b^{(i)}}, \tag{2}$$

where $W_b^{(i)}$ denotes the weight of the bracing system in iteration i, and $C^{(i)}$ indicates the corresponding

resulted compliance. The $PI^{(i)}$ is then the ratio of the performance measure in the ith iteration to the initial protomorph conditions. The optimum is then found by tracing the PI history. Such a method is called Performance-Based Optimization (PBO) by Liang et al. [14,16].

The same technique is employed in the present work, with the additional advantage that, by using this discrete approach, the reduction of strength in linear members due to buckling effects can also be taken into account, even via code-based relations. While the stiffness of a candidate member is not as small as in the case of continuum approaches, the assumptions of the sensitivity analysis may be weakened, making the discrete extension as an approximate intuitive method. In such cases, the PI trace curves are not expected to be very smooth. However, the emphasis and interest of this paper is on the effect of graph theoretical guidelines in improving design.

In this work, the cross sections of bracing members are taken to be pipe-shaped, so that by using such a code-based threshold for the ratio of diameter to thickness, design variables for each member can be reduced and converted to the sectional area. In this way, a unified method for having compact sections for stress response evaluations is obtained implicitly, satisfying such a constraint. Using the S.I. units and AISC-ASD-89 design code relations [23]:

$$\frac{h}{t} = \frac{2.36}{\beta.F_y}, \tag{3}$$

$$A = \frac{\pi}{4}.(h^2 - (h-t)^2), \tag{4}$$

where h, t and A denote the pipe section height, thickness and area and β is a safety factor, taken as 1 in this work.

In linear analyses, stress ratios can also be used as η^e, since the strain value of an axial member, in this case, is linearly proportional to its stress and the strain energy density is calculated by the product of these two linear proportional values. Moreover, the PI history is traced until there is no member to be checked for elimination. The following algorithm performs as a general optimization procedure in this work:

Algorithm 3:

1. Generate a proper protomorph as described in the previous section;
2. Initiate the sectional area of bracing members and set the iteration number; $i = 0$;
3. Analyze the structural model to find the resulted strain energy density, γ^e, and stress ratio, r_e, for structural members and the overall performance index for the current iteration step, i;
4. Increase the iteration number by one, $i = i + 1$;
5. Determine the proper member removal measure, η^e, for each bracing member, based on the results of the analysis and any additional desired topological considerations;
6. Make a sorted list of the member numbers in ascending order of their η^e values;
7. Select the first member in the list as the current candidate to be checked for elimination;
8. Check for the topological constraints after temporary removal of this candidate;
   a. If all such constraints are satisfied, i.e. the candidate member is not marked as Undeletable, go to Step 9;
   b. Otherwise:
      i. Ignore the current candidate for elimination;
      ii. If there is no candidate unchecked in the list, go to Step 11;
      iii. Select the next member in the sorted list as the new candidate;
      iv. Go to Step 8.
9. Eliminate the candidate member from the current structural model;
10. If any bracing member is still remained, go to Step 3;
11. Identify the local optima in the PI trace history and its global maximum;
12. Announce the layout corresponding to the maximal PI as the primary optimum of the problem.

The secondary optimum can also be considered among the found local PI optima to be checked for any additional constraint or objectives which are not explicitly included in the recent procedure, such as the sparsity of frame openings from an architectural point of view.

GRAPH THEORY ASSISTANCE FOR TOPOLOGY OPTIMIZATION

The topological considerations applied in Steps 5 and 8 of the main optimization algorithm are satisfied by graph theoretical operators as follows.

Nodal Ordering and Modifying the Member Removal Criteria

In many cases, such as safe seismic design and fundamental eigenvalue maximization, the priority of stiffening is given to lower story levels of the structure, i.e. the nearer members to the supports. This concept, as a topological objective, can be incorporated into

the optimization procedure using the following graph ordering:

Algorithm 4:

1. Generate the protomorph structure and associate with it the corresponding graph;
2. Determine the support nodes as MSRT roots;
3. Generate an MSRT from the selected roots and order the nodes of the graph as they enter this MSRT. These order numbers for each node will be the graph theoretical distance between that node and the support nodes;
4. Reverse this nodal ordering, such that the farthest nodes from the roots be assigned the least order number, i.e. zero;
5. Associate to any bracing member the sum of the new nodal orders of its end nodes, i.e. the reversed distance from supports;
6. Normalize the resulted member ordering numbers so that their maximum becomes unity;
7. For each bracing member, e, use the normalized ordering number, μ^e, to modify the computed removal measure, η^e, in Step 8 of Algorithm 3, as: $\eta^e = \eta^e \times \mu^e$.

When any other root nodes are selected for example in nodes of a specific story level, the same algorithm can be used to topologically arrange the stiffening bracing distributions around those nodes.

Topological Control of the Lateral Load Path

The function of bracing axial members in a frame is to act as a lateral load resisting system when the original moment frame connections are not efficient for this purpose. Hence, in an optimal design, it is desirable to minimize the contribution of beams or columns in resisting lateral loads, thus maximizing the contribution of bracing members instead. One way to seek such a goal is to provide lateral load paths from their exertion points to the supports, which is possible only through bracing members. This topological constraint can be satisfied during the optimization process by utilizing graph theoretical concepts through the following algorithms.

Checking Connectivity of the Bracing Graph

In Step 8 of Algorithm 3, run the following steps of Algorithm 5 to check the connectivity of any load path through bracing members:

Algorithm 5:

1. Consider the bracing graph associated with the selected layout;
2. Select the support locations as root nodes;
3. Run up to Step 3 of Algorithm 4 to determine the nodal distances from roots in the protomorph graph to be used as priority numbers for PMSRT in the next step;
4. Grow a PMSRT in the current bracing graph. Due to the priorities employed from the previous step, it is then called an Upward Multiple Shortest Route Tree, UMSRT;
5. If there is any bracing member in the current layout not included in the generated PMSRT, mark the candidate member as Undeletable;
6. Return to Algorithm 3.

Preserving the Lateral Load Path to at Least one Support Node

For every lateral nodal load, follow these following steps:

Algorithm 6:

1. Select the load exertion point as a SRT root node;
2. Run up to Step 4 of Algorithm 4 to determine the reversed nodal distances from roots in the protomorph graph to be used as priority numbers for PMSRT in the next step;
3. Grow a PMSRT in the current bracing graph. Due to the priorities employed in the previous step, it is then called a Downward Shortest Route Tree (DSRT);
4. If the DSRT hits a support node, back track the path toward the root node using the generated graph theoretical vectors; StemOf/BudOf;
5. Consider the path graph obtained as the lateral load path to the support and mark the bracing elements in this path as Undeletable;
6. Return to Algorithm 3.

After repeating the above algorithm for all lateral loads, check if the candidate member in Step 8 of the main optimization procedure is marked Undeletable.

Preserving the Path from the Supports to the Lateral-Load Nodes

Run the following subroutine once, just after generation of the initial protomorph/ground structure in Step 1 of the main optimization routine

Algorithm 7:

1. Consider the structural support locations as root nodes;
2. Run up to Step 3 of Algorithm 4 to determine the nodal distances from roots in the protomorph graph

to be used as the priority numbers for PMSRT in the next step;

3. Grow a PMSRT in the current bracing graph. Due to the priorities employed from the previous step, it is then called an Upward Multiple Shortest Route Tree, (UMSRT);
4. Mark every nodal load exertion node as initially-covered if it is covered by the PMSRT in Step 2.

Then, in Step 8 of the main optimization (Algorithm 3) after temporary removal of the candidate member from the bracing layout run the following subroutine:

Algorithm 8:

1. Consider the structural support locations as root nodes;
2. Grow an UMSRT on the current bracing graph from the selected roots;
3. If any of the load-point nodes is marked initially-covered, due to Algorithm 7, but is not labeled via the current UMSRT, then mark the candidate member as Undeletable in the current elimination iteration;
4. Return to Algorithm 3.

More restricted versions will be obtained by repeating the steps of the two previous algorithms separately for any support node.

Preserving the Path from Each Lateral-Load Node to all the Supports

As a subroutine in Step 8 of Algorithm 3, for every lateral nodal load, run the following steps:

Algorithm 9:

1. Select the load exertion point as a root node;
2. Before elimination of the candidate member in Algorithm 3 do the following:
   a. Grow a DSRT from the selected root node;
   b. Check for any support node that is included in the generated DSRT. If so, mark it as an initially-covered support by the selected load-node.
3. Temporarily eliminate the candidate member and do the following:
   a. Grow a DSRT from the selected root node;
   b. For any support node, if it is marked as initially-covered but is not included in the generated DSRT, mark the candidate member as Undeletable. If not, check the next support node.
4. Repeat the previous steps until no lateral node is remained unchecked;
5. Return to Algorithm 3.

Further Considerations and Smoothing the Achieved Optimal Design

Due to practical considerations, the output of the main optimization algorithm may require more finalizing modifications. For example, when a lateral load path hits an auxiliary intermediate common node between two bracing members, they are desired to be in the same line in order to reduce the extra lateral force transfer to that beam [18]. In such a case, a partial geometry optimization for this node may be applied by the following routine:

Algorithm 10:

1. Consider the bracing graph associated to the obtained layout;
2. Find any node having degree number 2 in the bracing graph and mark it as a candidate for geometry modification;
3. Calculate the new location of the candidate node on the corresponding beam to preserve the fact that the 2 bracing members adjacent to this node are geometrically in the same line;
4. Modify the coordinates of (move) the candidate node to its new location, if no other node is available.

Another practical consideration is to limit the number of bracings in every frame opening, due to architectural requirements. This may be simply applied to Step 8 of the main optimization routine (Algorithm 3), via the steps of this subroutine:

Algorithm 11:

1. Temporarily eliminate the candidate member from the bracing graph;
2. Distinguish every frame opening as a minimal length cycle subgraph in the frame graph;
3. If the number of bracing diagonals with their ends belonging to the treated cycle is less than the pre-assigned number, mark this candidate member as Undeletable;
4. Return to Algorithm 3.

In order to determine the nested minimal length cycles in a graph, refer to [19].

The layout obtained at the end of the main optimization procedure may be conformed toward a

concentric bracing system at a superior level by Algorithm 12 as follows:

Algorithm 12:

1. Decompose the nodal set of the protomorph employed to:
   a. Main nodes at the location of beam-column joints;
   b. Auxiliary intermediate nodes in beams generated through construction of a proper protomorph;
   c. Support nodes.
2. If the degree of any auxiliary node in the bracing graph is one, then consider it as a root node and do the following:
   a. Grow an SRT on the frame graph from this root in order to find the nearest main node to it, regarding graph theoretical distance. This main node will be at the end of a column;
   b. Find the bracing member incident to the auxiliary node and if its other end is not on the same column, substitute the auxiliary end of the member with the nearest found main node in the frame.

The result of the latter topological operator is, hereinafter, called a Concentric Super Bracing System (CSBS). In this regard, the traditional CBSs are, in fact, subsets of possible CSBSs in a braced frame.

ILLUSTRATIVE EXAMPLES

Example 1: 2-Bay 6-Story Frame with 162-Member Protomorph

As a comparative benchmark example, a 2-bay 6-story frame is considered as illustrated in Figure 4. The unbraced moment frame with fixed supports in half dimensions was originally optimized for minimum weight by Huang and Arora [12] to satisfy the stress constraints, according to the AISC design code under uniform floor loads of 14.59 kN/m and point loads of 40.05 kN at story levels as a wind load. The 14 resulted section groups in Figure 4 are listed as: W8 × 21, W8 × 28, W10 × 26, W12 × 26, W14 × 26, W10 × 19, W10 × 17, W8 × 10, W12 × 19, W12 × 14, W14 × 22, W16 × 26, W16 × 31 and W24 × 62.

A more severe wind load condition (wind speed = 210 km/h) was then imposed by Mijar et al. [13] to this unbraced frame. This frame did not satisfy the code requirements and had to be braced. Consequently, they employed the Voigt-Reuss material mixing rule to optimize the bracing layout retrofit for this example and then explored some baseline problems including the minimization of compliance under the constraint of

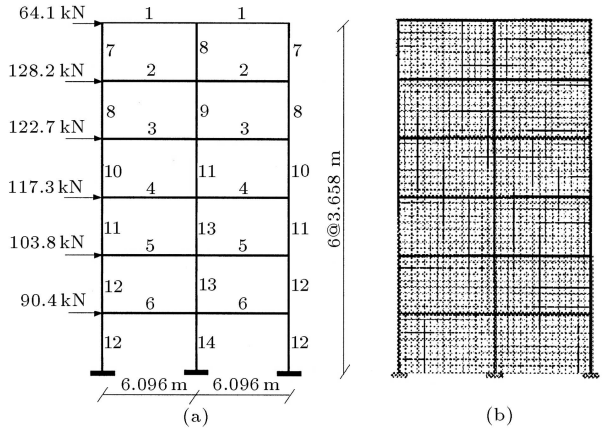

Figure 4. (a) Member groups of the 2-bay frame under 14.59 kN/m floor loads and wind loading; (b) Finite element design domain used in continuum formulations [13,14].

a fixed volume fraction in the designable domain. They finally interpreted the result of this problem with 50% reduction in wind load to standard W-sections, based on equal mass M (Figure 5). Liang et al. [14] applied their method to this problem using reverse formulation, i.e. minimization of bracing weights subjected to the mean compliance constraint. In both of these continuum approaches, the ground structures were formed by subdividing frame openings as topological design domains into 1620 plane stress finite elements of a uniform thickness of 0.0254 m (Figure 4b).

Here, the deterministic method described in the previous section, based on PBO, is adopted under the same loading state, with a 50% reduced reversible wind load. In order to obtain rather comparable results, the initial section areas for all bracing members were selected, such that the resulted bracing weights were equal to the initial weight of the continuum FEM design domain in the literature [13,14]. Consequently, the performance index (PI) is calculated during the elimination iterations of the main routine (Algorithm 3),

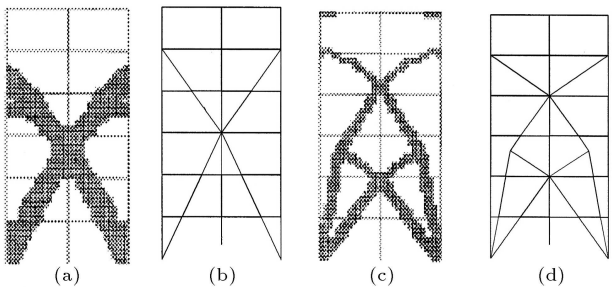

Figure 5. (a) Results of continuum optimization methods; (b) the interpreted model obtained by Voigt-Reuss material mixing formulation with 30% volume fraction constraint [13], (c) and (d) Conceptual solution by performance-based optimization with 22% volume fraction and its interpreted layout [14].

combined with a variety of other prescribed algorithms and, by tracing the resulted history of PI, global and local optima are identified. The protomorph structure of Figure 2c is selected for this example with 108 bracing diagonals and 54 frame members, which are considerably less than the number of initial elements employed in continuum approaches. Due to symmetry, the maximum number of elimination iterations will be at most 54.

The first attempt is purely the implementation of PBO for the discrete skeletal model. As shown in Figure 6, the maximum PI obtained as 1.94 belonged to iteration 47 with the bracing layout of Figure 7a. This layout led to a 0.025 m maximum sideway displacement for 13.7 percent of the initial bracing weights in the selected protomorph. It should be noted that the bracing graph of Figure 7b is not connected and consists of 2 components. Therefore, transmission of the lateral loads from any bracing in the upper component to the supports requires the contribution of the beams or columns of the frame and increases their stress response. As a result, the stress constraints were not completely satisfied by this design.

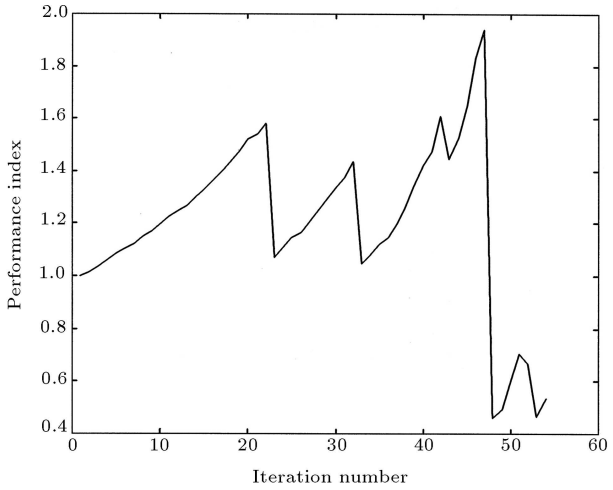

Figure 6. The PI history obtained by Algorithm 3 for a 2-bay 6-story frame example and its global maximum at iteration 47.

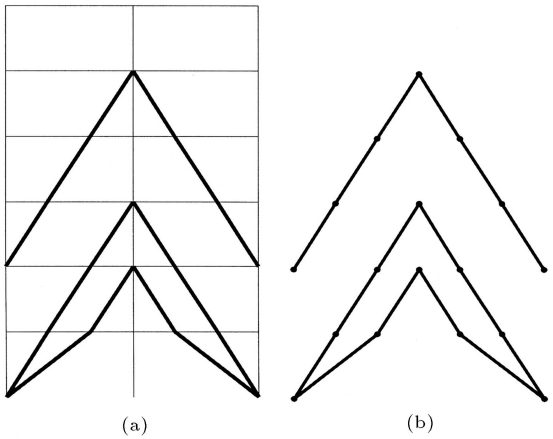

Figure 7. (a) The maximal PI bracing layout obtained by a pure form of Algorithm 3; (b) Two components of the associate bracing graph.

In order to preserve spanning all the frame levels by the bracing layout, Algorithm 11 is incorporated as the second attempt. This time, the PI history curve is smoother with greater maximum with respect to the pure implementation of PBO. Regarding the combination of Algorithm 11 with Algorithm 3, the least architectural limitations belonged to iteration 49, whereas there was no new candidate member unchecked. After this, the procedure was continued, in order to see if a better design could be achieved when releasing this topological constraint (Figure 8). By limiting the ratio of the thickness to diameter of the pipe section considered as the bracing section areas, their local buckling could be prevented.

Further study of the resulted topology is possible by decomposing the layout obtained into the frame graph and the bracing graph. Figure 9c demonstrates the result of a contraction imposed on this bracing graph. The original connected layouts, whose contracted forms are analogous to ordinary bracing units, are called Super Bracings [15], such as concentric V-type and eccentric X-type super bracings (see Figure 9b). In this regard, any ordinary bracing type can be considered as a subset of the super bracing.

Note that, due to the selection of a practical protomorph and since the corresponding graph has auxiliary nodes on the beams, the resulted super bracing members may intersect beams at those points. In such a case, the corresponding brace-to-beam joints are modeled as hinge (moment-free) connections. The capability of exact connection modeling in a brace-to-column/beam is another advantage of the current

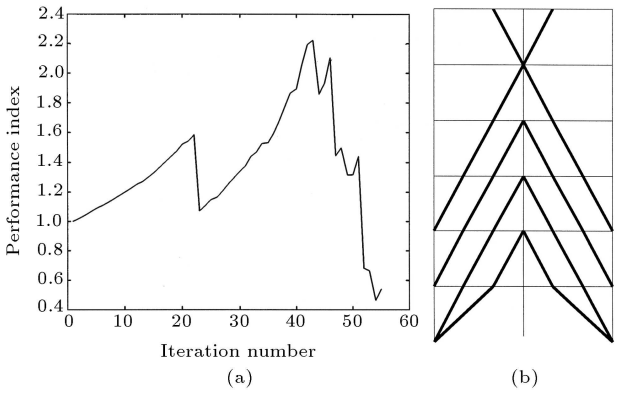

Figure 8. (a) The PI history for Example 1 obtained by Algorithm 11 up to iteration 49 then continued by only Algorithm 3; (b) Layout correspondent to the maximum PI.

discrete optimization method for skeletal structures over continuum approaches.

Figure 10 shows the effect of modifying removal criteria, η^e, by extracted member ordering in Algorithm 4, μ^e. As can be realized, in this case, the last layout of Algorithm 11 is guided to shift toward the supports. However, the resulted bracing graph is again disconnected.

The effect of preserving the connectivity of the bracing graph as a topological constraint, during optimization, is demonstrated in Figure 11. In this case, the global optimum achieved has the maximal performance index of 2.07, requiring 11.5% of the total initial bracing weight, leading to a sideway of 0.024 m at the top story. This time, any lateral load imposed to a bracing end can be transmitted through the connected bracing graph to the supports.

In order to preserve such a path, via a bracing graph, for support nodes to all the lateral loads, Algorithms 7 and 8 are incorporated (Figure 12). In Figure 13 the location of the lateral loads in one of the symmetric loading cases is denoted by arrows. As depicted in bold lines in Figure 13b, all the lateral-load

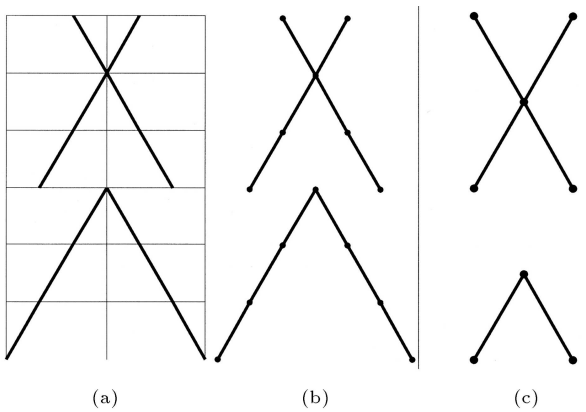

Figure 9. (a) Layout of iteration 49 by Algorithm 11; (b) The corresponding bracing layout consists of 2 super-bracings of X-type and V-type; (c) Contraction of path graphs ended at the node on the symmetric line has transformed the super bracing graphs into traditional forms of bracing.

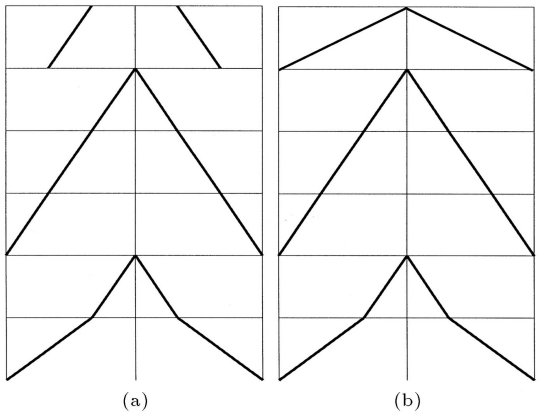

Figure 10. (a) The layout of last iteration 49 generated during mixed Algorithms 11 and 4 in the main routine; (b) Modified layout by Algorithm 12.

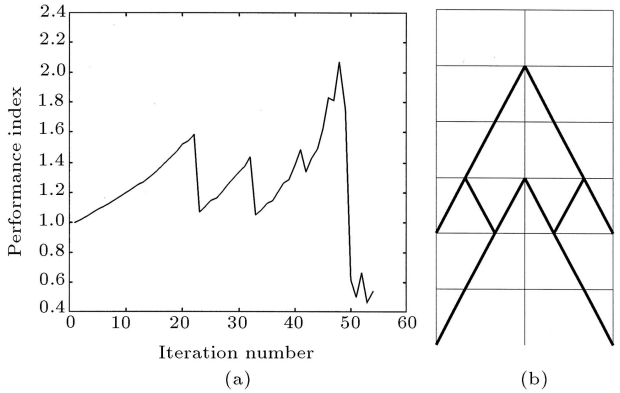

Figure 11. (a) PI history; (b) The optimal layout achieved by incorporating Algorithm 5.

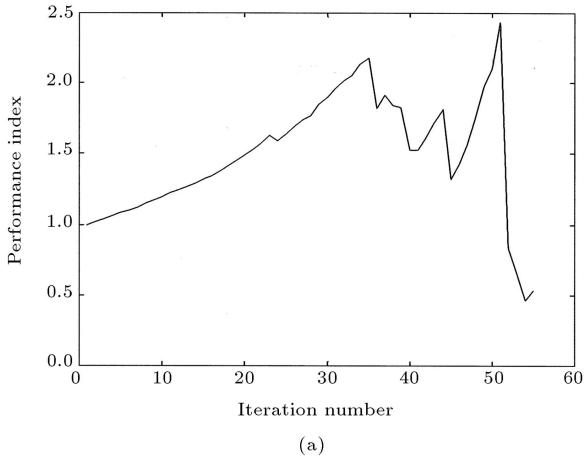

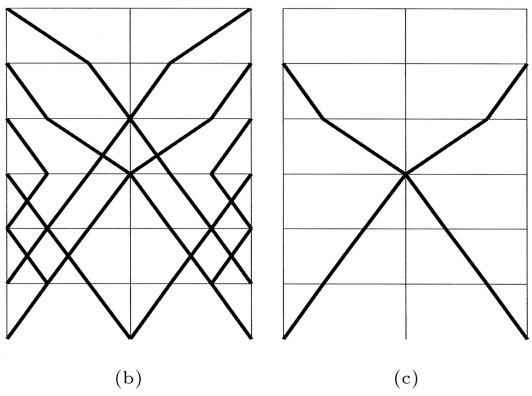

Figure 12. (a) PI history of Algorithm 8 up to iteration 40 and then continued by Algorithm 3; (b) The optimal layout achieved by incorporating Algorithm 8 at iteration 39; (c) The maximal PI layout obtained in the tag part of the trace continued by pure Algorithm 3 at iteration 51.

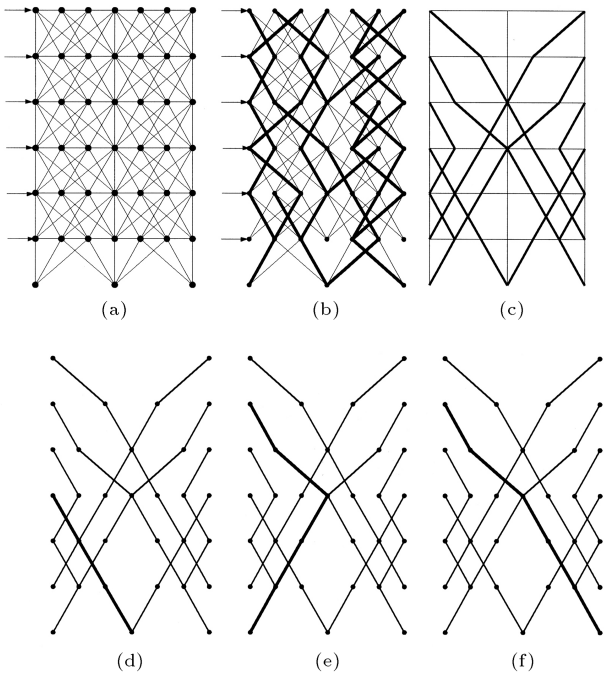

Figure 13. (a) The exertion points of lateral loads in the selected protomorph; (b) An UMSRT grown in Algorithm 7 from the support nodes in the bracing graph of the protomorph and covered lateral-load points; (c) Optimal layout by imposing Algorithm 8 to main discrete PBO; (d) The load path from the exertion point in the 3rd story to the support node as a path subgraph in the bracing graph of the optimal layout; (e) and (f) Two possible paths from the load exertion point in the 5th story to the supports.

exertion nodes, except one at the level of the 1st story, are initially covered by the UMSRT grown from the 3 support nodes in the bracing graph of the selected protomorph. It should be noted that Algorithm 3, for any lateral load, only preserves the load path to at least one support node, rather than all of them. For example, Figure 13 shows such a path in the suboptimal bracing graph of iteration 39 from the load-point at the 3rd story to only the middle support node, while there are 2 load paths to either of the corner supports for the lateral load imposed at the level of the 5th story.

The performance index at the end of Algorithm 8, iteration 40, was greater than unity, which is the PI associated with the selected protomoph. It seems a good idea to continue tracing PI by implementation of pure Algorithm 3, starting from the ending layout of Algorithm 8 as a new protomorph. In this tag of the trace, the 1st local optimum belonged to a sparser layout of iteration 44 (Figure 14a). Smoothing it by Algorithm 10, the bracing system of Figure 14b obtained, which includes 2 X-type and 1 V-type super bracings, leading to minor is changes in the displacement response. As a global optimum, the layout of iteration 51 was achieved with an even greater performance index than the suboptimal layout of the 1st part of the trace. However, it led to a greater displacement at the top story and greater maximum stresses. This layout was further modified by Algorithm 10, as shown in Figure 15b. The topology obtained is, in fact, an X-type super bracing that exactly complies with the interpreted layout of Mijar et al. [13] (Figure 5).

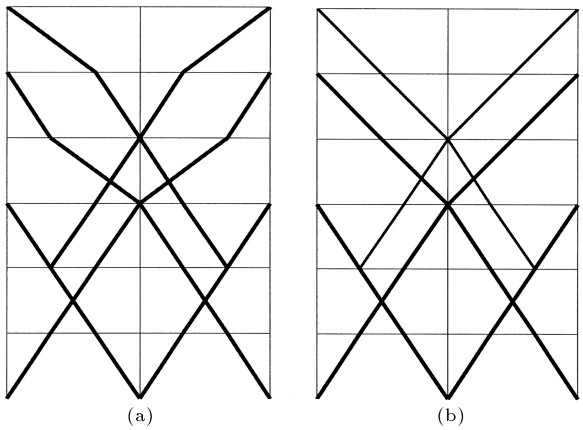

Figure 14. (a) Topology achieved at iteration 44 of Algorithm 8 followed by Algorithm 3; (b) The corresponding smoothed bracing layout by Algorithm 10.

Applying Algorithm 9, load paths from their exertion points to the supports are preserved during the optimization. From every lateral load-point, a DSRT is grown to identify the support nodes it covers. The optimal design, due to Algorithm 9, belongs to the layout shown in Figure 16b. In order to illustrate such a technique, load-paths from a sample exertion point at the 5th story are depicted in Figure 17. Compared to the previous discrete algorithms and even continuum methods, more support nodes are covered in the load paths captured by Algorithm 9 and, consequently, less stress/displacement responses are achieved, as shown in Table 1.

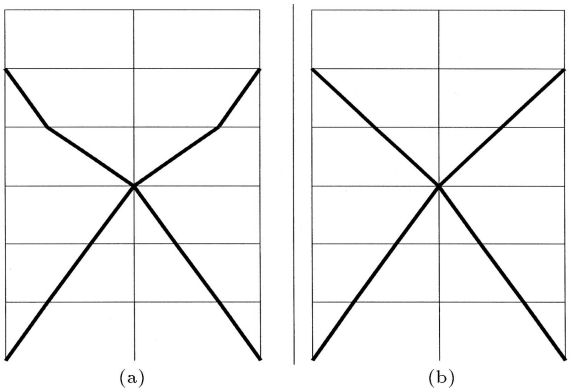

Figure 15. (a) Global maximum PI topology achieved at iteration 51 of Algorithm 8 followed by Algorithm 3; (b) The corresponding smoothed bracing layout by Algorithm 10.

Table 1. Comparative results of sample achieved designs for 50% reduced wind load.

Layout Design	Design Weight Ratio (%)	Performance Index	Maximum Displacement (m)	Half* Number of Major Elimination Iterations	Average Number of Bracing Diagonals in Each Frame Opening
Figure 5a [13]	30	0.32	0.035	567	0.8
Figure 7a	13.7	1.94	0.025	47	1.3
Figure 8b	20.3	2.22	0.015	43	2
Figure 14a	20.8	1.81	0.010	44	2
Figure 15b	8.7	2.45	0.028	51	0.8
Figure 16b	33.8	1.61	0.008	36	3.1
Figure 16c	26.7	1.84	0.009	41	2.5

* Due to symmetric elimination of less efficient members.

As the eliminating process is continued, by applying pure Algorithm 3, the 1st new local optimum in the PI trace is obtained at iteration 41, while its corresponding bracing layout satisfied all the stress and displacement constraints (Table 2). The maximal PI belongs to the layout of Figure 16d.

Example 2: A 2-Bay 6-Story Frame with 186-Member Protomorph

In order to allow ordinary X-bracings for optimal design, the protomorph of Figure 2d is considered as the next attempt, regarding a full wind load case. This case is treated by Algorithm 9 followed by Algorithm 11 and then Algorithm 3 (Figure 18). In the maximal performance design of Figure 18b, there are paths from the positions of all the lateral loads to support nodes, while traditional X-bracings are only encountered in the 1st story.

Tracing such a design sequence for sparser topologies due to architectural objectives, the layout of iteration 55, as a second local optimum, and then the smoothed layout of Figure 18d can be concerned. It is realized that in the continuation of the optimization trace, ordinary bracings have been gradually disappeared and only super bracings with long diagonal paths were remained. This indicates that super bracings are more efficient layouts for resisting lateral loadings. As an example, 3 X-type and 2 V-type super bracings are recognized in the layout of iteration 55 (Figure 18c). The sparser layout of Figure 18d, including 2 nested X-type and one V-type super bracings, required only 12.8% of the initial bracing weights to produce an even better performance than in the previous continuum works (Table 2). In the considered examples, super bracings generally provided the shortest continuous load paths to the support nodes rather than traditional bracing units.

DISCUSSION AND CONCLUSIONS

In the present work, the application of PBO is extended to the topology optimization of discrete skeletal bracing members in frame structures. Despite the conceptual designs in continuum methods, such a discrete approach resulted in a sequence of design possibilities practically applicable to the bracing layout. The main method is further improved by means of a number of graph theoretical operators, in order to handle a variety of topological constraints and objectives, such as the connectivity of lateral load paths via bracings toward the supports.

In order to study the topology of the design domain, the structure is decomposed into the frame graph

Table 2. Comparative results of sample designs for full wind load.

Layout Design	Design Weight Ratio (%)	Performance Index	Maximum Displacement (m)	Half* Number of Major Elimination Iterations	Average Number of Bracing Diagonals in Each Frame Opening
Figure 5a [13]	30	0.32	0.070	567	0.8
Figure 5c [14]	22	1.15	0.024	632	1.5
Figure 18b	26.7	1.84	0.009	41	2.5
Figure 18d	12.8	1.99	0.016	60	1.3

* Due to symmetric elimination of less efficient members.

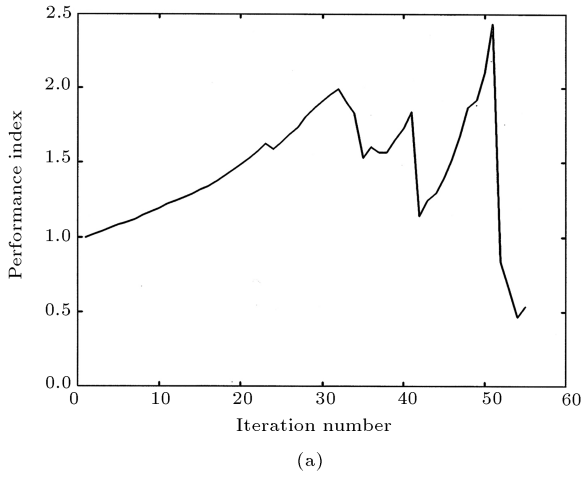

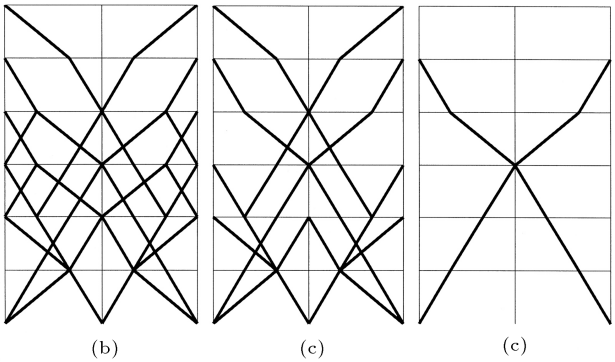

Figure 16. (a) PI history of Algorithm 8 up to iteration 40 and then continued by Algorithm 3; (b) The local optimal layout at iteration 39; (c) the layout of iteration 41; (d) The maximal PI layout at iteration 51.

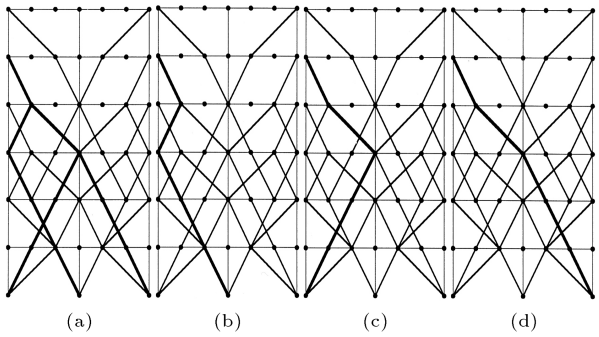

Figure 17. (a) A sample DSRT grown in the bracing graph from the left lateral-load exertion point in the 5th story (in bold lines), (b), (c) and (d) The resulted load paths to each of the support nodes.

and the bracing graph. Graph theoretical operators enable the optimization procedure to control lateral load paths and enforce special topological constraints. As a result, the performance index history has been upgraded in a smoother manner. The selected protomorph allowed the formation of traditional bracing patterns, however, the optimization resulted in new

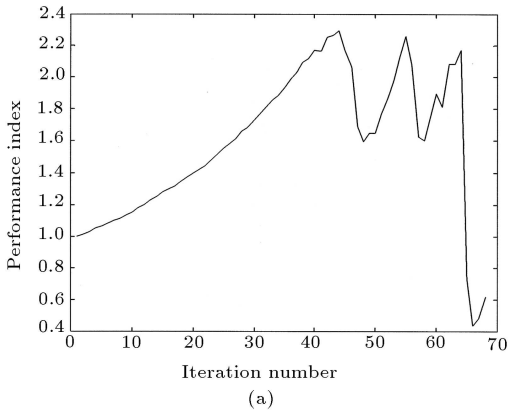

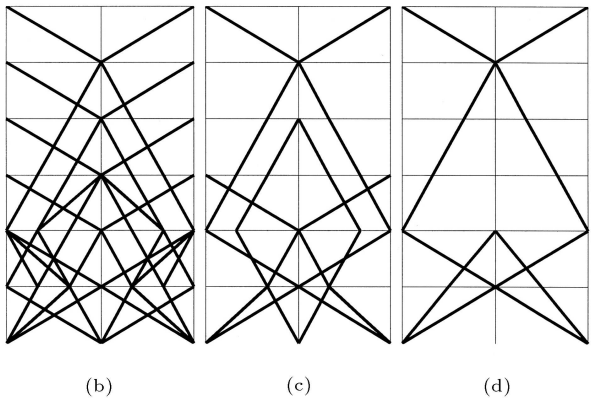

Figure 18. (a) PI history for 100% wind load generated by Algorithm 9 up to iteration 49 followed by Algorithm 11 up to iteration 62 and then continued by Algorithm 3; (b) The optimal layout achieved at iteration 44; (c) Sparser layout at iteration 55; (d) Smoothed layout of iteration 60.

more efficient bracing layout. Such layouts are further studied and classified as super bracing systems.

Since graph theoretical operators only deal with the topology and connectivity of structural frameworks, they are by no means limited to static linear elastic analysis and can easily be extended to other cases, such as material/geometric nonlinear analyses. Applying a specific graph theoretical algorithm corresponds to the implementation of a particular topological constraint/objective. Therefore, this can be considered as a new problem formulation, however, not analytically assessed.

The bracing layout of the maximal PI may be considered as a good optimum. However, some further practical and architectural objectives may lead to another design among the subsequent local optima. Most of the optima in the treated examples led to concentric super bracing systems, considered as the most efficient bracing layouts for stiffening a building frame. Theoretically, it is shown that such bracing layouts can provide continuous lateral load paths to the supports. This matter is more important in the

seismic/wind retrofit cases, while the contribution of original frame members in undergoing lateral loading effects is to be minimized.

The results in Tables 1 and 2, show the superiority of the present discrete optimization method for controlling the displacement response within considerably less iterations and costs for bracing weights. By means of the developed algorithms, the selected result at any iteration of the optimization process can further be modified, due to practical or analytical considerations, such as the partial geometry smoothing of super bracing diagonals or exchanging an eccentric SBS by a concentric type. Finally, the graph theoretical operations are shown to be suitable and powerful tools in applying various topological constraints and objectives to the optimization procedure, which cannot be directly formulated by analytical relations.

REFERENCES

1. Taranath, B.S. *Structural Analysis and Design of Tall Buildings*, McGraw-Hill Inc., New York (1998).
2. Ghasemi, M.R., Hinton, E. and Wood, R.D. "Optimization of trusses using genetic algorithms for discrete and continuous variables", *Engineering Computations*, **3**, pp. 272-301 (1999).
3. Kaveh, A. and Kalatjari, V. "Topology optimization of trusses using genetic algorithm force method and graph theory", *International Journal for Numerical Methods in Engineering*, **58**, pp. 771-791 (2003).
4. Kaveh, A. and Kalatjari, V. "Size/geometry optimization of trusses by the force method and genetic algorithm", *ZAMM*, **84**(5), pp. 347-357 (2004).
5. Tang, W., Tong, L. and Gu, Y. "Improved genetic algorithm for design optimization of truss structures with sizing, shape and topology variables", *International Journal for Numerical Methods in Engineering*, **62**(13), pp. 1737-1762 (2005).
6. Gulay, G. and Boduroglu, H. "An algorithm for the optimum design of braced and unbraced steel frames under earthquake loading", *Earthquake Engineering and Structural Dynamics*, **18**, pp. 121-128 (1989).
7. Gallagher, R.H. and Gellatly, R.A. "Automated minimum weight design of framework structures", *International Symposium on the Use of Computer in Structural Engineering*, University of Newcastle, UK (1966).
8. Kim, C.K., Kim, H.S., Hwang, J.S. and Hong, S.M. "Stiffness-based optimal design of tall steel frameworks subject to lateral loads", *Structural Optimization*, **15**, pp. 180-186 (1998).
9. Kameshki, E.S. and Saka, M.P. "Genetic algorithm based optimum bracing design of non-swaying tall plane frames", *Journal of Constructional Steel Research*, **57**, pp. 1081-1097 (2001).
10. Mueller, K.M., Liu, M. and Burns, S. "Fully Stressed Design of Frame Structures and Multiple Load Paths", *Journal of Structural Engineering*, **128**(6), pp. 806-814 (2002).
11. Di Sarno, L. and Elnashi, A.S. "Bracing systems for seismic retrofitting of steel frames", *Proceeding of 13th World Conference on Earthquake Engineering*, Vancouver, Canada (2004).
12. Huang, M.-W. and Arora, J.S. "Optimal design of steel structures using standard sections", *Structural Optimization*, **14**, pp. 24-35 (1997).
13. Mijar, A.R., Swan C.C., Arora J.S. and Kosaka I. "Continuum topology optimization for concept design of frame bracing systems", *Journal of Structural Engineering*, **124**, pp. 541-550 (1998).
14. Liang, Q.Q., Xie, Y.M. and Steven, G.P. "Optimal topology design of bracing systems for multistory steel frames", *Journal of Structural Engineering*, **126**(7), pp. 823-829 (2000).
15. Kaveh, A., Mofid, M. and Shahrouzi, M. "Parametric study of various bracing layouts for the seismic retrofit of steel frames", *Proceeding of Fifth International Conference on Civil Engineering*, (in Farsi) Ferdowsi University of Mashhad, Iran, pp. 347-355 (2000).
16. Liang, Q.Q., Xie, Y.M. and Steven, G.P. "A performance-based optimization method for topology design of continuum structures with mean compliance constraints", *Computer Methods in Applied Mechanics and Engineering*, **191**, pp. 1471-1489 (2002).
17. Hsu, Y.-L., Hsu, M.-S. and Chen, C.-T. "Interpreting results from topology optimization using density contours", *Computers and Structures*, **79**, pp. 1049-1058 (2001).
18. Kim, H.I. and Goel, S.C. "Upgrading of braced frames for potential local failures", *Journal of Structural Engineering*, **122**(5), pp. 470-475 (1996).
19. Kaveh, A., *Optimal Structural Analysis*, John Wiley, 2nd Ed., Tounton, Somerset (2006).
20. Kaveh, A., *Structural Mechanics: Graph and Matrix Methods*, 3rd Ed., Research Studies Press, John Wiley, Somerset, UK (2004).
21. Mazzolani, F.M. "Design of seismic resistant steel structures", *10th European Conference on Earthquake Engineering*, Balkema, Rotterdam (1995).
22. Ebrahimi Farsangi, H. and Salajegheh, E. "Topological optimization of double layer grids using genetic algorithms", *Proceeding of the Fifth International Conference on Civil Engineering*, Ferdowsi University of Mashhad, Iran, pp. 45-54 (2000).
23. American Institute of Steel Construction (AISC), *Allowable Stress Design and Plastic Design Specifications for Structural Steel Buildings*, 9th Ed., Chicago, IL (1989).